Experimental and Monte-Carlo study of double-hump electron emission yield curves of SiO 2 thin films

Quentin Gibaru, Christophe Inguimbert, Mohamed Belhaj, Sarah Dadouch, Mélanie Raine, Damien Lambert, Denis Payan

Experimental and Monte-Carlo study of double hump electron emission yield curves of SiO_2 thin films

Q. Gibaru[1,2,3], C. Inguimbert[1,a)], M. Belhaj[1], S. Dadouch[1], M. Raine[2], D. Lambert[2], D. Payan[3]

[1]*ONERA-DPHY, 2 avenue E. Belin, 31055 Toulouse, France*

[2]*CEA, DAM, DIF - 91297 ARPAJON, France*

[3]*CNES, 18 av. E. Belin, 31401 Toulouse CEDEX, France*

In this work, we have made experimental measurements of multiple-hump electron emission yield (TEEY) curves on SiO_2 thin films. A Monte-Carlo electron transport model, published in Q. Gibaru, C. Inguimbert, M. Belhaj, M. Raine, and D. Lambert, Journal of Electron Spectroscopy and Related Phenomena **261**, 147265 (2022), has been developed to analyze the physical reasons of such atypical behavior. It is shown that the multiple-hump TEEY curves of thin dielectric layers are due to internal recombination effects. However, such kind of phenomena is demonstrated to be strongly correlated to the incident current density. This analysis reveals that, the double-hump TEEY curves observed commonly on insulators are also most probably a measurement artefact, tied to the operating parameters of the electron gun. A careful choice of experimental parameters can eliminate this artefact, by using a constant current density that is also low enough to limit recombination effects.

I. INTRODUCTION

The emission of secondary electrons by a material under electron irradiation is a phenomenon that is encountered in various applications. While this phenomenon can be used in electron microscopy to get an image, it is also the source of parasitic effects, such as the e-cloud effect in particle accelerators[1,2], or the charging mechanism of spacecrafts[3]. This phenomenon is generally quantified by the total electron emission yield (TEEY), which is the ratio of the total number of electrons exiting the material over the number of incident electrons. The TEEY is driven by various parameters, such as the electron energy, incident angle, surface chemistry and roughness… Nevertheless, the TEEY curves reported in the literature generally follow a standard behavior according to the electron energy. They are composed of a single hump with a maximum value at a given energy Emax, and two crossover energies E_{C1} and E_{C2} where the TEEY curve goes respectively above and below 1.

Several efforts have focused on the study of the TEEY of insulating materials, which require special considerations due to the charging phenomena [4–7]. Indeed, the emission (TEEY > 1) or absorption (TEEY < 1) of electrons by the dielectric target can respectively create a positive or negative charge in the material. This charge significantly alters the secondary electron process by generating an external electric field, which can modify the energy of incident electrons by either accelerating them toward the surface or by forcing their recollection. While the recollection of secondary electrons can be avoided by biasing the sample

holder or the collector, the creation of electron/hole pairs inside the material can also disturb the transport of electrons in the solid[8,9] and impact the secondary electron emission process. All these effects can thus significantly alter the TEEY of insulators, which could be subject to artefact measurements. It induces substantial complications for the experimentalist that do want to avoid such type of artefact in dielectric materials. Indeed, the charge buildup can increase or decrease the TEEY during the measurement. This means that for a same material, various TEEY values can be found depending on the measurement conditions. Several studies have reported experimental TEEY measurements on such samples that do not follow the standard behavior of TEEY[10–12]. The measured TEEY exhibit a double-hump shape, with the apparition of a TEEY local minimum between the two humps. This behavior has mainly been reported for SiO_2 thin film samples, although it has also been observed on other space-used dielectric materials.

A few explanations have been proposed for these observations. Ye et al.[13] have shown that the variation of the beam diameter could create double hump TEEY curves as an experimental artefact. However, these observations were made in the case of metallic samples with surface roughness structures of millimetric dimensions.

For dielectric materials, Hoffman and Dennison[14] proposed an explanation linked to external charging effects. However, other works[10–12] have also observed multiple hump TEEY curves on SiO_2 thin films of various thicknesses grown on a Si substrate. In these studies, the sample holder was negatively biased to avoid the recollection of secondary electrons, so that this behavior cannot be attributed to external field effects only.

Yi et al.[12] and Yu et al.[11] proposed that the local TEEY minimum can be removed by compensating the holes created in the SiO_2 layer by electrons tunneling from the Si layer. This is in agreement with other works that showed a link between the hole density and the TEEY[8,9]. They also proposed that the second TEEY maximum is due to enhanced compensation of the holes by electrons tunneling from the Si layer when the penetration depth of electrons is equal to the thickness of the SiO_2 thin film layer. On the other hand, Rigoudy et al.[10] suggested that a TEEY minimum instead appears under such conditions, where a conductive canal evacuates the secondary electrons from the SiO_2 layer under the effect of radiation induced conductivity. However, the local TEEY minimum appears in their measurements at the same incident energy for various SiO_2 thicknesses.

Notably, in these three studies, the TEEY local minimum was removed by a change of experimental parameters, such as increasing the positive bias of the collector[10] or the negative bias of the sample holder[12], or decreasing the incident current[11]. As a result, the apparition of the double hump TEEY curves could be linked to the conditions of measurement and could also be an experimental artefact.

In this work, we seek to further understand the conditions of appearance of the double hump TEEY curves on SiO_2 thin films, and to propose an explanation linked with the transport of electrons and holes in the material. First, we have made experimental measurements of the TEEY of SiO_2 thin films, and observed double-hump or even triple-hump TEEY curves depending on the measurement parameters. We then use a Monte-Carlo electron transport model to explain the apparition of the TEEY local minimum.

II. EXPERIMENTAL STUDY of DOUBLE HUMP TEEY CURVES

A. Experimental setup

The experiments were made with the DEESSE facility at ONERA[3], whose main characteristics are reminded below. The setup is composed of an ultra-high vacuum chamber (10^{-9} mbar), in which all measurements were made.

The TEEY was measured using samples of amorphous SiO_2 thin films from NEYCO, which were grown on Si using plasma growth. The samples have a thickness of 20 nm and a width of 5 cm. The samples were first heated for 48 hours to reduce the surface contamination by desorption. The temperature of the sample holder was set to 200°C. The temperature (RT) was increased from 23°C (RT) to 200°C using 5°C/min ramp. Thereafter the temperature was kept contestant at +/- 0.2° C during 48h using homemade temperature regulation system controlled by a LabVIEW program. The cooling down to RT is reached few hours after switching off the heater. Using the in-situ Auger analysis capabilities of the facility, the chemical composition of the surface has been checked to ensure that it has been properly decontaminated. From this analysis, only a small amount of hydrocarbon contamination remains (C_{KLL} Auger peak in Figure 1).

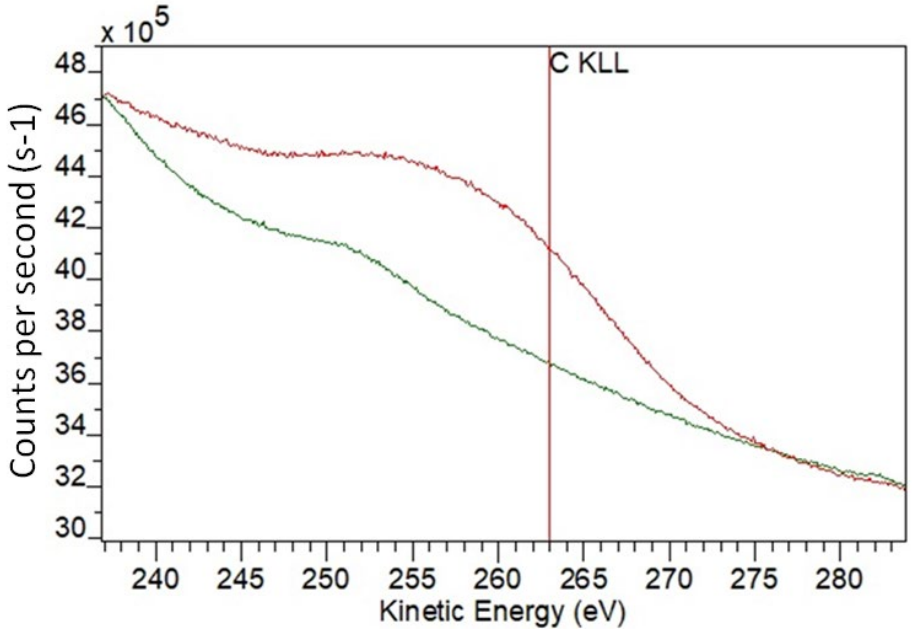

FIG. 1. Auger Electron Spectra (AES) in Counts Per Seconds (CPS). C_{KLL} pics are shown for the as received SiO2 surface (in red) and the in situ 48 heated at 200°C SiO2 samples (in green).

The TEEY measurement procedure is based on two measurements of the current flowing through the sample. By current conservation law, the incident current I_0, the emitted current I_E and the current flowing through the sample I_S follow the expression:

$$\boldsymbol{I_0 = I_E + I_S} \tag{1}$$

First, the sample holder is biased to a potential of +27 V. Due to the external electric field induced by the bias, practically all low energy electrons are recollected by the surface. The measured current I_S is very close to the incident current ($I_0 \cong I_S$). In a second step, the sample holder is biased to a -9 V potential, to prevent the recollection of secondary electrons which can be caused by the positive charging of the target. The current I_S measured in this case can be used to determine the emitted current using eq. (1) and the incident current I_0 obtained from the previous step: $I_E = I_0 - I_S$

Finally, the TEEY is given by the ratio of the emitted current over the incident current:

$$\boldsymbol{TEEY = \frac{I_E}{I_0}} \tag{2}$$

The target is irradiated by a 1 eV - 2 keV Kimball Physics ELG2 electron gun, in a defocused configuration (10 mm² to a few cm²) set at normal incidence. The beam spot area can be adjusted by changing the focus voltage F from 0 V to 1000 V, where a focus of 0 V is expected to produce a very broad beam spot (~ cm²), while a focus of 300 V gives a narrower beam spot (~ mm²).

The pulsing capabilities of the gun were used to send several pulses of incident current of 0.1 μA (0.1-1 μA/cm² current density) and 100 μs to 6 ms duration, with a 50 ms to 200 ms relaxation period between each pulse. This method is used in place of a continuous incident current to limit the effect of charging on the TEEY.

B. Double hump TEEY measurements on SiO_2 thin film sample

In Figure 2 below, the experimental results for the TEEY of SiO_2 thin films are shown. Each data point from 100 eV to 2 keV was obtained by averaging the TEEY from 10 pulses of 6ms spaced of 200ms. A first series of 10 pulses is sent with the sample biased to +27 V to measure the incident current I_0, then a second series of 10 pulses is sent with the sample biased to -9 V to measure the sample current I_S. In both cases, the current is averaged over the 10 pulses. The TEEY is then computed

using the equation (2). A focus voltage of 300 V was used. One can see the appearance of a local minimum of the TEEY around 1 keV. This is coherent with the other observations made on SiO_2 thin films, where a local minimum also appeared around 1 keV in the case of double-hump curves.

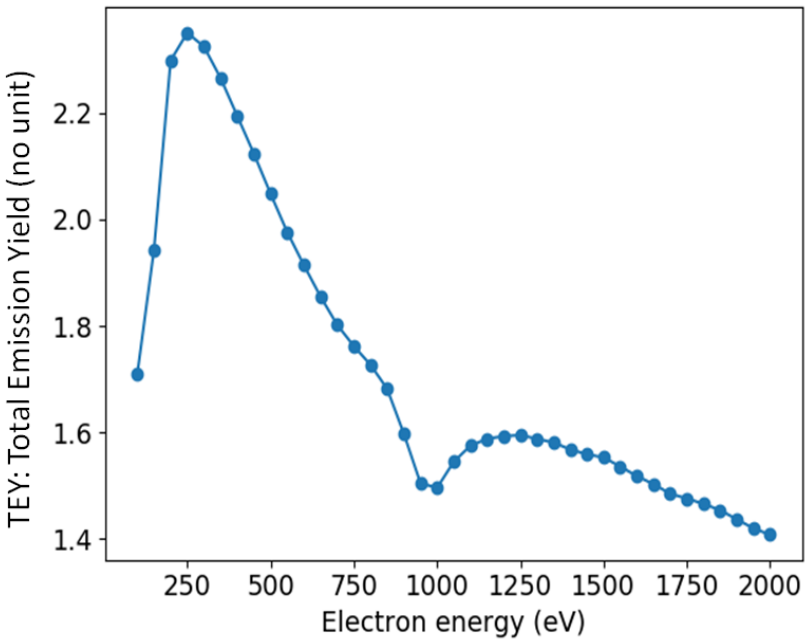

FIG. 2. Double hump TEEY of SiO_2 thin film sample measured at F = 300 V.

We have also made experimental TEEYs measurements using different values of focus voltage. The results are shown in Figure 3. If a broad beam is used (F = 0V), the maximum value of the TEEY increases from 2.3 to 2.7. Interestingly, in such a case, the local minimum of the TEEY has disappeared. Moreover, changing the focus voltage from 300V to 100V or 500V changes the position of the local minimum of the TEEY and its relative amplitude compared to the maximum TEEY. When a 100 V focus voltage is used, the local minimum is moved to 500 eV and has a higher variation compared to the max TEEY than at F = 300V. In the case of a 500V focus voltage, there is even a second local minimum that appears at 250 eV, with the local minimum around 1 keV that has been previously observed.

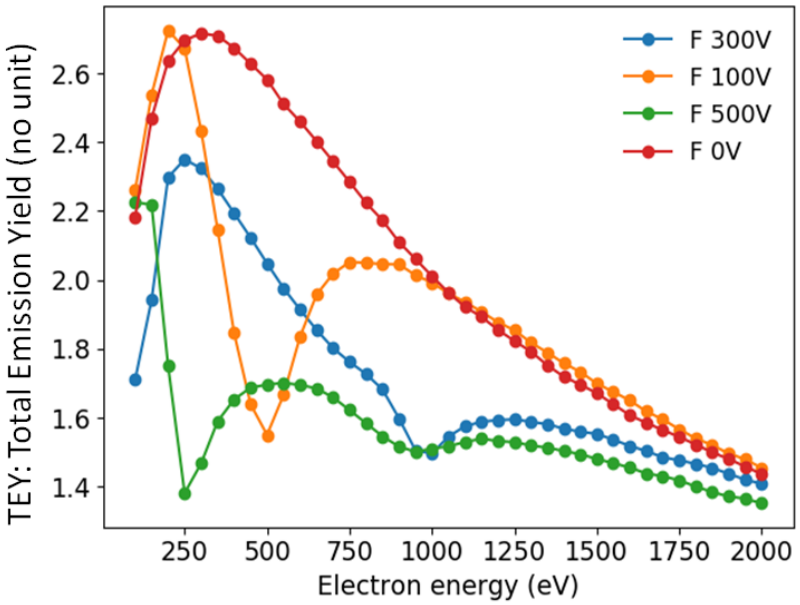

FIG. 3. Comparison of the TEEY curves obtained with different focus voltages

Finally, two TEEY measurements were made in DEESSE with a thin film sample of MgO using a focus voltage of 250 V. The results are given in Figure 4. Here again, we find at F 250V a double-hump TEEY curve with a local minimum at 900 eV, which is only slightly shifted compared to the minimum observed at 1 keV at a focus of 300 V. This local minimum is also eliminated if the focus is changed to 0V, as was the case for SiO_2. By changing the focus voltage, we were able to make appear or disappear a local minimum of TEEY on a different insulator, which demonstrates that this effect is not a property of SiO_2 alone. Given that we observe TEEY curves that are very similar to Figure 3, this points to physical processes which would be common to insulator thin films. On the other hand, this could also be linked to the protocol or parameters we use to measure the TEEY, because we obtain the same results on two different insulators but with the same measurement parameters.

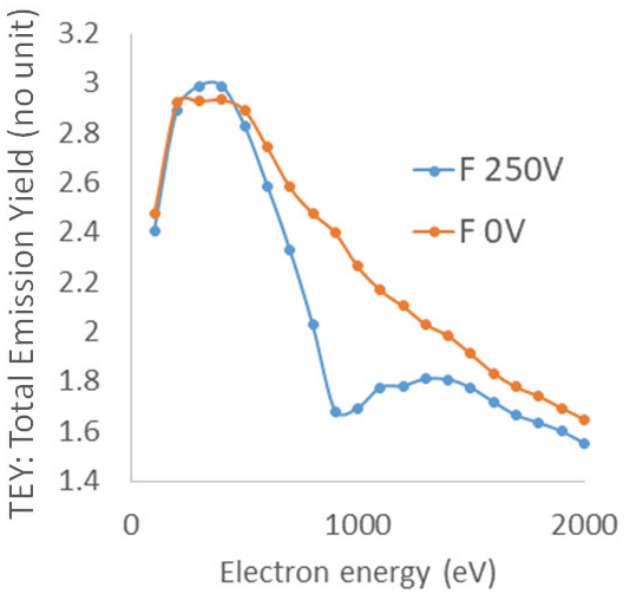

FIG. 4. Double hump TEEY of a MgO thin film sample measured at F = 250 V

C. Study of the current density of the incident beam

To understand the effect of these different beam parameters, we have first studied the evolution of the incident current, to see whether there was a dependence on the focus voltage and/or energy. The incident current for the focus voltages F = 100V, 300V and 500V are shown in Figure 5. One can see an increase of the incident current with energy, from a few tens of nA at 50 eV to 0.3 µA at 2 keV. However, this variation of the incident current is independent on the focus voltage, so that the three plots are superimposed. Given the significant variation of the position and amplitude of the TEEY local minimum, the variation of the incident current alone cannot explain the dependence of the TEEY on the focus voltage.

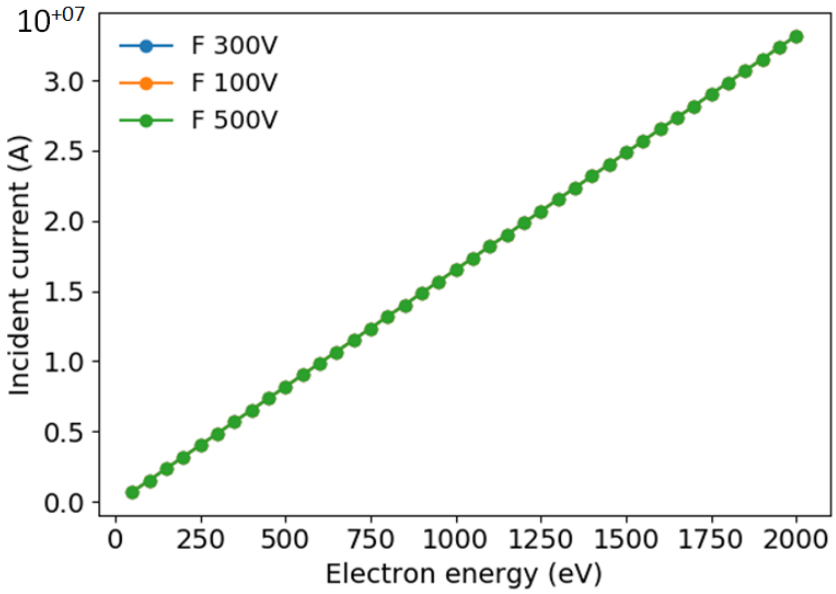

FIG. 5. Variation of the incident current with the focus voltage

The incident beam spot size has then been measured for different values of the focus voltage (0, 100, 300, 500 V). The measurements were made by using the electron gun on a 5 cm wide aluminum square plaque covered by sodium salicylate powder. As this powder is phosphorescent, this allows us to get an image of the spot size of the beam, which area can be measured. The measurements are shown in Figure 6. For the three focus voltages F = 100V, 300V and 500 V, there is a significant variation of the beam spot size with the electron energy. For instance, the area goes from 1.8 cm² at 300eV to 0.08 cm² at 1 keV for F = 300V. In the case of F = 100 V, the beam area goes up to 13 cm² at 2 keV (the graph has been cut at 2 cm² for legibility). No data is provided for a focus voltage of 0V, because the beam surface was wider than the area covered by the phosphorescent powder (> 25cm²) at all energies.

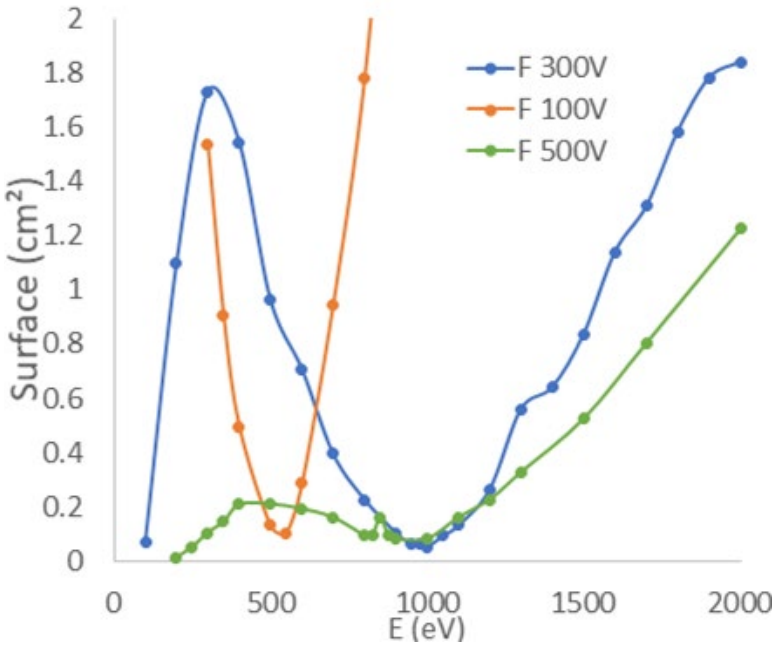

FIG. 6. Variation of the beam area with the focus voltage and electron energy

From Figure 6, one can see a direct correlation between the area irradiated by the beam and the shape of the TEEY curves of Figure 3. The local minimum of TEEY appears at the same energy than the minimal spot size, which is about 0.1 cm² for F = 100V at 550 eV, F = 300V and F = 500V at 1 keV, and 1mm² for F = 500V at 200eV. One can also see that the presence of two minimal area points at F = 500 V (250 eV and 1 keV) creates a triple-hump TEEY curve with two local minimums at the same energies. The beam area is also equal to or lower than 0.2 cm² at F = 500V on a large energy range (200 eV to 1.2 keV). This leads to a TEEY that is constantly lower than with the other focus voltages, except at the local minimum of beam area at 500 eV for F = 100V. Such variations of beam surface with electron energy were also reported in other works[13].

D. Study of the temporal evolution of the TEEY

Rather than sampling the whole TEEY curve averaged over several pulses, it is also possible to sample the evolution of the TEEY for a given energy after each pulse. In this section, we compare the time evolution of the TEEY for the energies and focus voltages where a TEEY minimum appears, with the evolution of the TEEY at the same energy but using a wider beam (F = 0V). The currents were not averaged over the pulses but were sampled for each individual pulse of 6 ms, following the two steps from section 2.2.

The experimental results are shown in Figure 7. For the energies and focus voltages combinations where the beam area is equal to or below 0.2 cm² (300 eV at F 500 V, 500 eV at F 100 V and F 500 V, and 1 keV at F 500 V and F 300 V), the TEEY

is immediately lowered after one pulse compared to the broader beams. For 300 eV and 500eV electrons, this lowering stabilizes after 10 to 15 pulses, while for 1 keV electrons the TEEY does not seem to evolve after the first pulse. This reduction of the TEEY is due to the recombination of secondary electrons with holes[9]. However, when the beam area is greater than 1 cm², the TEEY is much higher and has little to no decrease with time. This significant variation of the TEEY depending on the focus is coherent with the apparition of the local TEEY minimums in Figure 3.

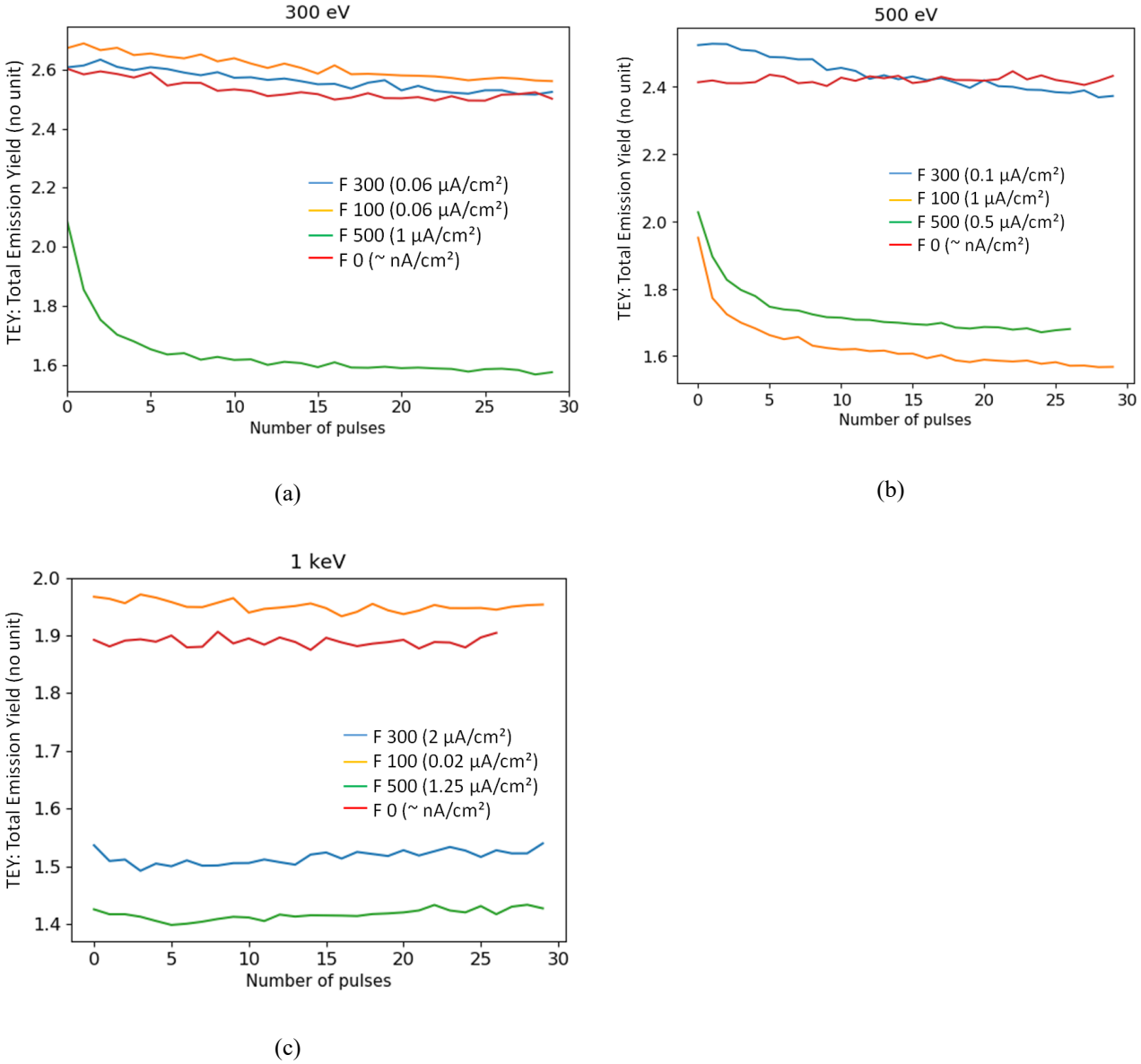

FIG. 7. Evolution of the TEEY in time with the number of pulses, depending on the incident energy and focus voltage (a) for 300 eV incident electrons, (b) for 500 eV, and (c) for 1 keV

There is a systematic shift between the TEEY curves that were obtained at the same energy and beam area, for instance at 500 eV between F 500 V and F 100 V, which have a beam area of 0.2 cm² and 0.1 cm². The same type of shift is found for the wide beam curves, for instance at 1 keV between F 100 V (4 cm²) and F 0V (> 25 cm²). In all cases, the TEEY curve that is lower corresponds to the measurement that was made later. In previous work[9], we have shown that the presence of residual deeply trapped holes in the sample may cause a shift of the measurements. This could be the source of the error observed here.

III. MONTE CARLO SIMULATION OF DOUBLE HUMP TEEY CURVES

A. Study of the effect of current density

To understand the effect of the current density of the electron beam on the evolution of the TEEY with time, we have used a Monte-Carlo simulation model. This code is based on the MicroElec[15–18] module of GEANT4[19], which in its currently available version can simulate the electron transport in SiO_2 and compute the electron emission yield without charge effects. In a previous work[9], a Monte-Carlo charging simulation model was developed, which can simulate the transport of holes and drift electrons generated by the incident electron cascade. The model, which is detailed in ref[9], can simulate the effect of charging on the electron emission of SiO_2 thin films, and can reproduce the experimental TEEY data for an incident current density of 10 µA/cm².

It has been previously demonstrated that the TEEY is gradually reduced following the creation of holes at the surface of the material, and the recombination of secondary electrons with these holes. This observation was made in the case of a beam surface of 0.1 cm², by using pulses of 100 µs separated by 50 ms to get a better time resolution. In the present work, a similar decrease of the TEEY induced by recombination was observed in Figure 7 at the local beam surface minimums (0.1-0.2 mm²) and using longer pulse lengths. However, when the beam area was a few cm² wide or larger, no decrease of the TEEY was observed.

In this work, this Monte Carlo model has been extended to study the influence of the current density. As this is a 1D model in depth and the objective is to understand a 2D surface effect, an empirical approach was used. This empirical approach can be justified by comparing the radius of an electron cascade (roughly 10 nm, Figure 8) with the beam area (up to several cm²). Indeed, if we want to have an accurate 3D mesh, it would need to have cells with an area that is not larger than the size of a cascade. This would lead to a mesh with 10^{+12} cells, which would require excessive computation time and resources.

From the incident current I_0, we can calculate the number of electron impacts after a given time τ by:

$$N_E(\tau) = I_0 \tau / e \quad (3)$$

Where e is the charge of an electron. The total area of the material where electron cascades have been created after τ is the product of the number of electrons $N_E(\tau)$, with the area of an electron cascade:

$$S_C = \pi r_C^2 \quad (4)$$

Where r_C is the radius of an electron cascade taken from the incident electron's point of impact. This radius can be extracted from the Monte-Carlo simulations, the data is given in Figure 8. In the simulations, the cascade radius r_c ranges from a few nm at 100 eV to a few tens of nm above 1 keV, following a behavior that is very similar to the extrapolated range of low energy electrons[20]. However the radius was measured without simulating the drift of the charge carriers generated in the electron cascade, which will increase its spread. To take the drift into account, the value of r_c that was used in the computation of the surface of the cascade was increased by 5 nm, which is an approximation of the length that can be traveled by a hole through a few hopping events before another electron hits the same area.

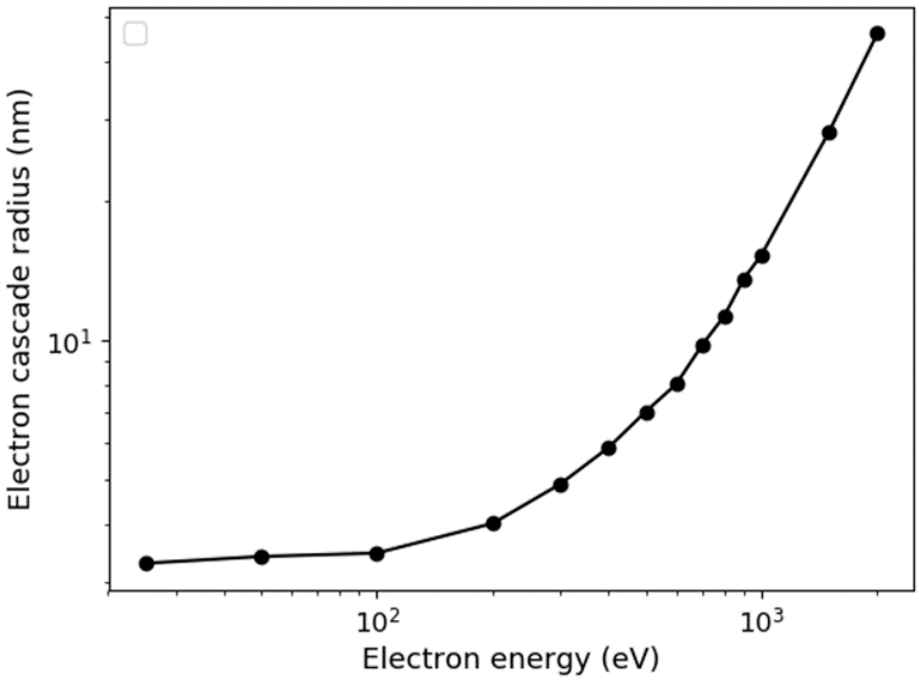

FIG. 8. Simulation results of the electron cascade radius in SiO_2 for different incident energies

From this, we can compute the proportion of the material surface filled with electrons and holes resulting from the electron cascades. It is simply expressed by the number of electrons $N_E(\tau)$ times the surface of a cascade, divided by the beam area. This gives the following overlap factor, where the incident current density J_0 appears:

$$\%_{Overlap}(\tau) = \frac{S_C N_E(\tau)}{S_B} = \frac{S_C}{e} J_0 \tau \quad (5)$$

This factor, illustrated in Figure 9, corresponds to the probability that an incident electron arrives in an area where another electron cascade was previously generated. In this case, the two cascades overlap, and the secondary electrons created in the new electron cascade can interact with the holes created by the previous cascade. However, if the electron arrives in an area that is still free of charges after τ, the electron cascade will not be affected by recombination with the charges created by the previous electrons.

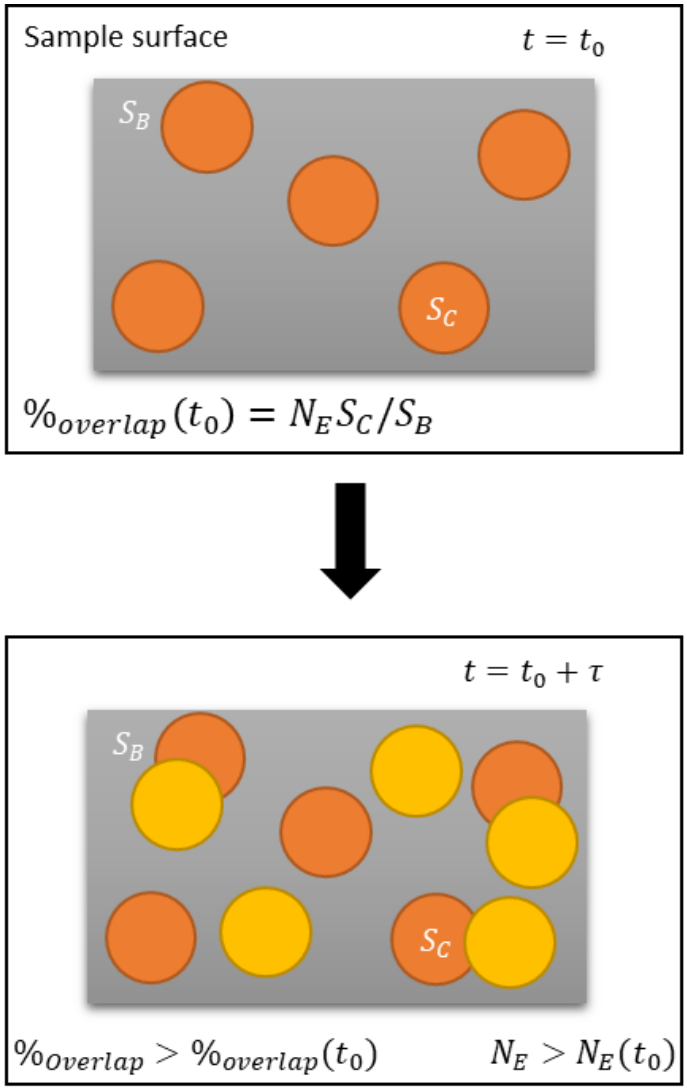

FIG. 9. Illustration of the evolution of the overlap factor with time

In the Monte-Carlo model, the trapping and recombination mean free paths λ_T and $\lambda_{e\text{-}h}$ depend on their respective capture cross section σ. They also respectively depend on the density of free traps N_F or the densities of trapped charges N_h and N_e:

$$\boldsymbol{\lambda = \frac{1}{\sigma N}} \quad (6)$$

In the simulation, our 1D model assumes that the charge densities N_h and N_e are uniform on the whole surface, and the capture mean free paths will always depend on the same charge density. However, this is only true if the current density is high enough, so that the electron cascades are uniformly distributed and an incident electron is guaranteed to arrive in an area filled with charges. Indeed, if a particle is created in a region where all traps are free, the charge densities should be empty. To take this into account, the overlap factor is used to compute an effective charge density $N_{eff}=\%_{overlap}(\tau)xN$ which is used in the computation of the mean free paths. The overlap factor is computed after each simulation time step τ. This factor is capped at 100%, which is the limit condition where the whole surface is covered by electron cascades.

Using an incident current of 1 µA as in ref.[9], the TEEY of 300 eV electrons was simulated in an attempt to qualitatively reproduce the experimental results of Figure 7. The simulation results are shown in Figure 10. When the beam area is small and the current density is large (0.1cm², 10 µA/cm²), we observe a decrease of the TEEY due to recombination, which is coherent with the experimental measurements made with a narrow beam.

However, when the current density is lowered and the beam area is larger (1 cm², 1 µA/cm²), the TEEY has a higher value and a slower decrease. In this case, the incident electrons do not hit the sample as uniformly as with a 10 µA/cm² density (0.1 cm² beam area). Therefore, the electrons have a much higher chance of arriving in a region of the material that has not been irradiated before. Thanks to the overlap factor, the simulation can consider this phenomenon. Indeed, after 10 pulses of 6ms, the overlap factor is 26% at 1 µA/cm² (beam area of 1cm².). In comparison, the overlap factor reaches 100% after 4 pulses for a current density of 10 µA/cm² (0.1 cm² beam area). In consequence, for a wider beam the proportion of secondary electrons lost by recombination is lessened, which leads to a higher TEEY.

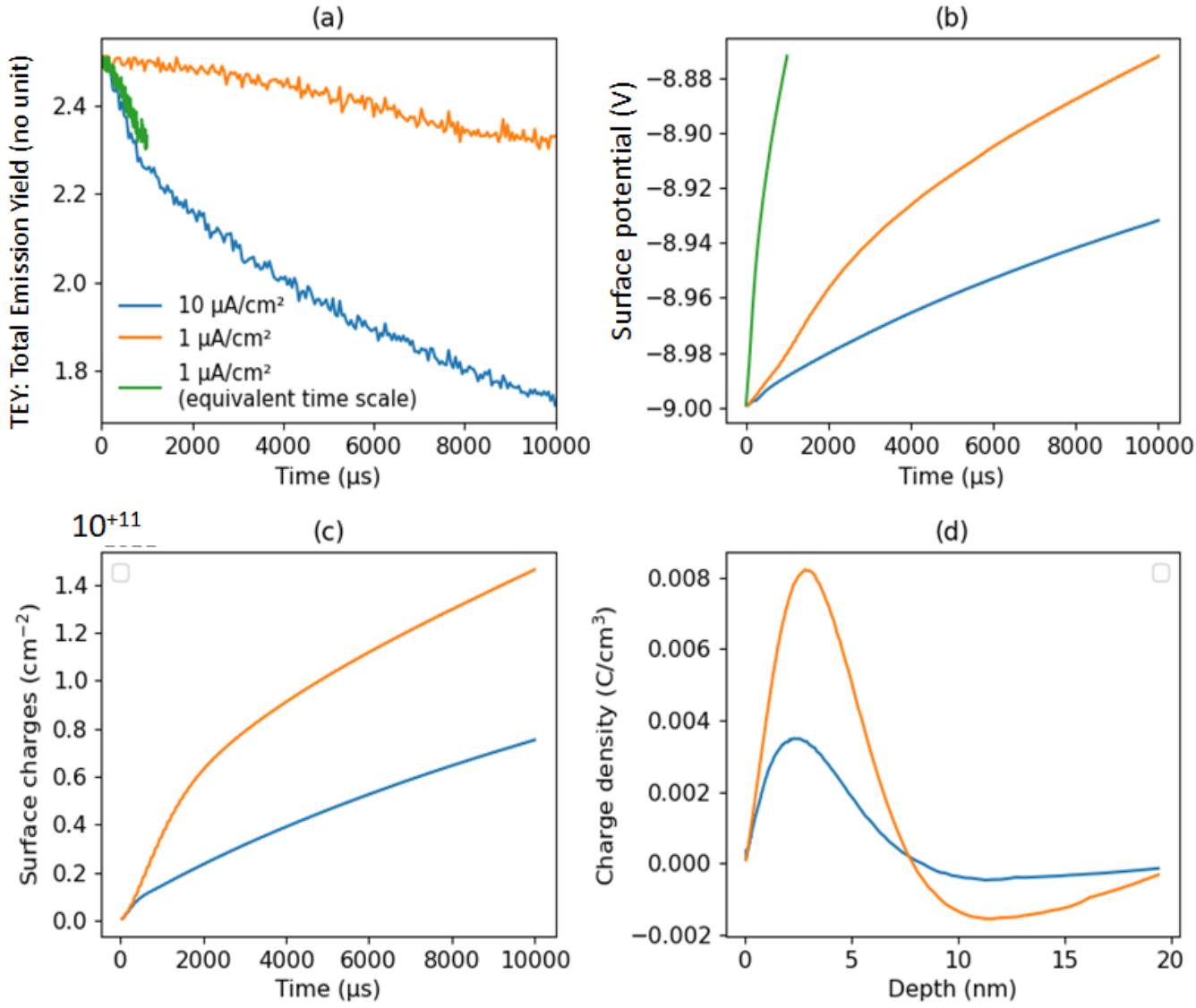

FIG. 10. Simulation of the TEEY of 300 eV electrons for a current density of 10 µA/cm² and 1 µA/cm²
(a) Evolution of the TEEY
(b) Evolution of the surface potential
(c) Evolution of the total surface charge density
(d) Charge density profiles at the end of 100 pulses

In Figure 10, the simulation results for 300 eV electron with a current density of 1 µA/cm² (beam surface of 1 cm²) have been plotted with the simulation results at 10 µA/cm² (beam surface of 0.1 cm²). The TEEY at 1 µA/cm² has also been plotted on a time scale reduced by a factor x0.1 to get an equivalent time scale compared to the TEEY at 10 µA/cm². The aim of this figure is to show that the two curves are not superimposed, and dividing the current density by 10 does not simply make the TEEY decrease 10 times slower. In fact, there is a competition between the time between two electron impacts at the same place, and the time needed for the holes to migrate by hopping. If the hole density at a given place is emptying faster than the time between two electron impacts, the decrease of the TEEY due to recombination should be less pronounced, which is what

happens at 1 µA/cm². At 10 µA/cm², the time between two electron impacts is short enough that a significant part of holes still remains and can capture the secondary electrons, which leads to the decrease of the TEEY. Depending on the material, this reduction of the TEEY may be more pronounced if the hole traps are deeper or more concentrated, or less pronounced if the holes are very mobile.

B. Simulation of the local TEEY minimums

Using the data from Figure 6, the simulation can also be used to reproduce the whole TEEY curve averaged over 10 pulses of 6 ms for the three focus voltages To do so, the TEEY has been simulated for 10 pulses of 6 ms with a 200 ms relaxation period. Each point of the TEEY curve is averaged over the 10 pulses, as in the experimental protocol used in section 2.2. The beam surfaces from the measurements in Figure 6 were used to compute the overlap factor, in order to simulate the effect of the focus voltage. In Figure 11, the simulation of the TEEY for focus voltages of 100, 300 and 500 V is displayed. By modifying the recombination probability according to the variation of current density, we can successfully simulate the apparition of the one or two local TEEY minimums that we had observed experimentally in Figure 3. Consequently, we are able to prove that the multiple hump TEEY curves are indeed linked to physical interactions of the electrons with the trapped charges. We have shown however that the physical interaction involved is the loss of secondary electrons by recombination, instead of RIC and the creation of a conductive canal. We have also demonstrated that these TEEY minimums are created by the variations of the current density with energy, which are themselves created by the variations of the beam surface with energy.

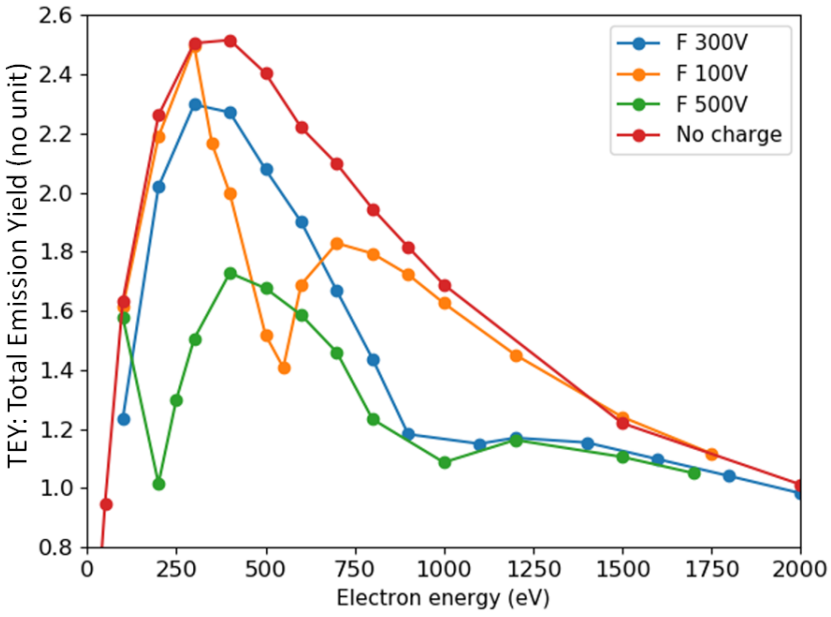

FIG. 11. Simulation of the TEEY curves obtained with different focus voltages

In Figure 12, a constant current density was used in the simulations for all energies (1 µA/cm² and 10 µA/cm², corresponding to 0.1 cm² and 1 cm²) and the TEEY was averaged over 100 pulses of 100 µs. In this case, the TEEY obtained at 10 µA/ cm² is lower than 1 µA/cm², as expected due to the decrease induced by the recombination. On the other hand, the TEEY at 1 µA/cm² is very close to the charge-less TEEY, with a maximum TEEY of 2.4 instead of 2.5 for the chargeless case. For both TEEY curves, there is no local minimum of TEEY appearing, since the current density is constant. With a narrower beam, the TEEY is lowered globally but not at select energies like in Figure 11. This demonstrates that the local TEEY minimums can be eliminated by working with a constant current density during TEEY experimental measurements. However, this current density should be low enough, to avoid a global lowering of the TEEY and a falsification of the data by the recombination effects. For SiO_2, this threshold appears to be below 1 µA/cm², but it may be different for other dielectrics with other charge transport properties.

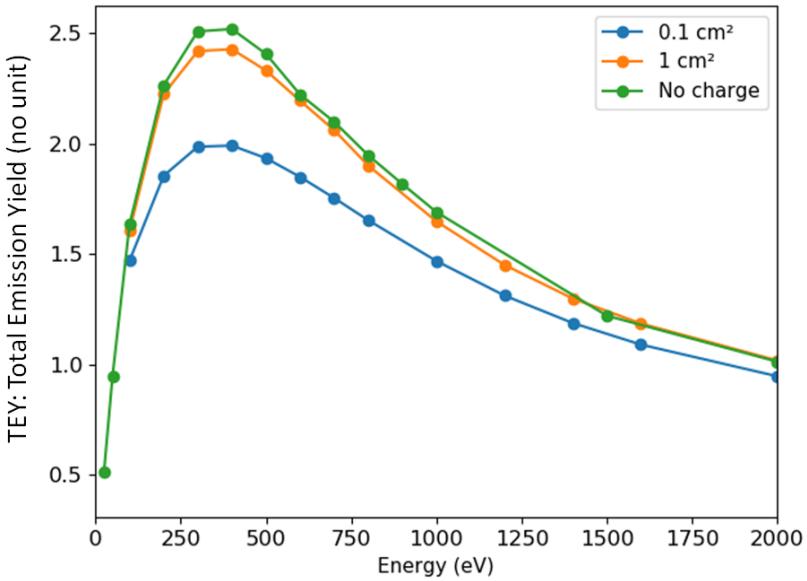

FIG. 12. Simulation of the TEEY averaged over 100 pulses of 100 µs with a constant current density

IV. CONCLUSION

In this work, we have used both experimental and simulated data, to prove that the multiple-hump TEEY curves of thin dielectric layers are indeed due to internal charging effects. Nevertheless, these are also created by the variation of the beam diameter, which depends on the choice of measurement parameters. Therefore, the double-hump TEEY curves observed on insulators are in fact a measurement artefact. A careful choice of experimental parameters can eliminate this artefact, by using a constant current density that is also low enough to limit recombination effects. In consequence, the experimental data given

in this work that were obtained with the lowest current density (Focus 0 V) should be the closest to the charge-less TEEY of the sample. With a very low current density, the great majority of incident electrons should hit regions of the sample that are free of charges. The charge transport models used in this work should also be valid for the transport of the electron-hole pairs created along the proton track in insulators. The MicroElec module of GEANT4, developed in this work for the ballistic transport of electrons, can also model the transport of protons. Thus, studying the same kind of artifact during proton irradiations is a subject of interest for future studies.

We have demonstrated here a significant influence of the current density on the TEEY of insulators. However, the current densities used in standard TEEY qualification for space-used dielectrics (1 μA/cm²) are much higher than the maximal current densities received by the materials on board of spacecrafts (10^{-10} A/cm² in a GEO orbit). Hence, the TEEY gathered during qualification in a controlled laboratory environment can be quite different from the TEEY of the material in its real conditions of usage. In consequence, it could be necessary to develop new experimental protocols, to obtain TEEY data that are more representative of the effective TEEY of dielectrics subjected to the space radiative environment.

ACKNOWLEDGMENTS

The authors would like to thank ONERA, CNES and CEA for providing the financial support for this work.

DATA AVAILABILITY

The data that support the findings of this study are available from the corresponding author upon reasonable request.

CONFLICT OF INTEREST

The authors have no conflicts to disclose

REFERENCES

[1] G. Rumolo, F. Ruggiero, and F. Zimmermann, Phys. Rev. ST Accel. Beams **4**, 012801 (2001).
[2] I. Bellafont, M. Morrone, L. Mether, J. Fernández, R. Kersevan, C. Garion, V. Baglin, P. Chiggiato, and F. Pérez, Phys. Rev. Accel. Beams **23**, 033201 (2020).
[3] N. Balcon, D. Payan, M. Belhaj, T. Tondu, and V. Inguimbert, IEEE Transactions on Plasma Science **40**, 282 (2012).
[4] J. Cazaux, Journal of Electron Spectroscopy and Related Phenomena **176**, 58 (2010).
[5] J. Cazaux, Journal of Electron Spectroscopy and Related Phenomena **105**, 155 (1999).
[6] M. Belhaj, T. Tondu, V. Inguimbert, B. Elsafi, S. Fakhfakh, and O. Jbara, Nuclear Instruments and Methods in Physics Research Section B: Beam Interactions with Materials and Atoms **270**, 120 (2012).
[7] M. Belhaj, T. Tondu, V. Inguimbert, P. Barroy, F. Silva, and A. Gicquel, J. Phys. D: Appl. Phys. **43**, 135303 (2010).
[8] M. Belhaj, T. Tondu, and V. Inguimbert, J. Phys. D: Appl. Phys. **42**, 145306 (2009).
[9] Q. Gibaru, C. Inguimbert, M. Belhaj, M. Raine, and D. Lambert, Journal of Electron Spectroscopy and Related Phenomena **261**, 147265 (2022).
[10] C. Rigoudy, K. Makasheva, M. Belhaj, S. Dadouch, G. Teyssedre, and L. Boudou, Journal of Applied Physics **130**, 135305 (2021).
[11] S. Yu, T. Jeong, W. Yi, J. Lee, S. Jin, J. Heo, J.M. Kimb, and D. Jeon, Appl. Phys. Lett. **79**, 3281 (2001).
[12] W. Yi, T. Jeong, S. Yu, J. Lee, S. Jin, J. Heo, and J.M. Kim, Thin Solid Films **397**, 170 (2001).
[13] M. Ye, P. Feng, D. Wang, B.-P. Song, Y.-N. He, and W.-Z. Cui, Chinese Phys. B **28**, 077901 (2019).
[14] R. Hoffmann and J.R. Dennison, IEEE Transactions on Plasma Science **40**, 298 (2012).
[15] Q. Gibaru, C. Inguimbert, P. Caron, M. Raine, D. Lambert, and J. Puech, Nuclear Instruments and Methods in Physics Research Section B: Beam Interactions with Materials and Atoms **487**, 66 (2021).
[16] M. Raine, M. Gaillardin, and P. Paillet, Nuclear Instruments and Methods in Physics Research Section B: Beam Interactions with Materials and Atoms **325**, 97 (2014).
[17] M. Raine, M. Gaillardin, and P. Paillet, Nuclear Instruments and Methods in Physics Research Section B: Beam Interactions with Materials and Atoms **325**, 97 (2014).
[18] A. Valentin, M. Raine, M. Gaillardin, and P. Paillet, Nuclear Instruments and Methods in Physics Research Section B: Beam Interactions with Materials and Atoms **287**, 124 (2012).
[19] J. Allison, K. Amako, J. Apostolakis, P. Arce, M. Asai, T. Aso, E. Bagli, A. Bagulya, S. Banerjee, G. Barrand, B.R. Beck, A.G. Bogdanov, D. Brandt, J.M.C. Brown, H. Burkhardt, Ph. Canal, D. Cano-Ott, S. Chauvie, K. Cho, G.A.P. Cirrone, G. Cooperman, M.A. Cortés-Giraldo, G. Cosmo, G. Cuttone, G. Depaola, L. Desorgher, X. Dong, A. Dotti, V.D. Elvira, G. Folger, Z. Francis, A. Galoyan, L. Garnier, M. Gayer, K.L. Genser, V.M. Grichine, S. Guatelli, P. Guèye, P. Gumplinger, A.S. Howard, I. Hřivnáčová, S. Hwang, S. Incerti, A. Ivanchenko, V.N. Ivanchenko, F.W. Jones, S.Y. Jun, P. Kaitaniemi, N. Karakatsanis, M. Karamitros, M. Kelsey, A. Kimura, T. Koi, H. Kurashige, A. Lechner, S.B. Lee, F. Longo, M. Maire, D. Mancusi, A. Mantero, E. Mendoza, B. Morgan, K. Murakami, T. Nikitina, L. Pandola, P. Paprocki, J. Perl, I. Petrović, M.G. Pia, W. Pokorski, J.M. Quesada, M. Raine, M.A. Reis, A. Ribon, A. Ristić Fira, F. Romano, G. Russo, G. Santin, T. Sasaki, D. Sawkey, J.I. Shin, I.I. Strakovsky, A. Taborda, S. Tanaka, B. Tomé, T. Toshito, H.N. Tran, P.R. Truscott, L. Urban, V. Uzhinsky, J.M. Verbeke, M. Verderi, B.L. Wendt, H. Wenzel, D.H. Wright, D.M. Wright, T. Yamashita, J. Yarba, and H. Yoshida, Nuclear Instruments and Methods in Physics Research Section A: Accelerators, Spectrometers, Detectors and Associated Equipment **835**, 186 (2016).
[20] Q. Gibaru, C. Inguimbert, M. Belhaj, M. Raine, and D. Lambert, Applied Surface Science **570**, 151154 (2021).